*J Neurophysiol* 94: 821–832, 2005.
First published March 30, 2005; doi:10.1152/jn.01049.2004.

# Temperature Affects Voltage-Sensitive Conductances Differentially in Octopus Cells of the Mammalian Cochlear Nucleus

**Xiao-Jie Cao and Donata Oertel**
*Department of Physiology, University of Wisconsin, Madison, Wisconsin*

Submitted 6 October 2004; accepted in final form 30 March 2005

**Cao, Xiao-Jie and Donata Oertel.** Temperature affects voltage-sensitive conductances differentially in octopus cells of the mammalian cochlear nucleus. *J Neurophysiol* 94: 821–832, 2005. First published March 30, 2005; doi:10.1152/jn.01049.2004. Temperature is an important physiological variable the influence of which on macroscopic electrophysiological measurements in slices is not well documented. We show that each of three voltage-sensitive conductances of octopus cells of the mammalian ventral cochlear nucleus (VCN) is affected differently by changes in temperature. As expected, the kinetics of the currents were faster at higher than at lower temperature. Where they could be measured, time constants of activation, deactivation, and inactivation had $Q_{10}$ values between 1.8 and 4.6. The magnitude of the peak conductances was differentially affected by temperature. While the peak magnitude of the high-voltage-activated $K^+$ conductance, $g_{KH}$, was unaffected by changes in temperature, the peak of the low-voltage-activated $K^+$ conductance, $g_{KL}$, was reduced by half when the temperature was lowered from 33 to 23°C ($Q_{10} = 2$). Changing the temperature changed the kinetics and the magnitude of the hyperpolarization-activated mixed cation conductance, $g_h$, but the changes in magnitude were transient. The voltage sensitivity of the three conductances was unaffected by temperature. The action of temperature on these conductances is reflected in the resting potentials and in the shapes of action potentials.

## INTRODUCTION

Temperature has long been known to affect electrical excitability. Hodgkin and Huxley showed that action potentials in squid axons are briefer and smaller at higher than at lower temperatures and that these differences in shape are the consequence of the sensitivity to temperature of the rates at which $Na^+$ and $K^+$ conductances are activated and deactivated ($Q_{10} = 3.0$) (Hodgkin and Huxley 1952a,c). The influence of temperature has been studied in squid axons, where the electrical activity is well described by two voltage-sensitive conductances, each well described by relatively few, temperature-dependent, rate constants. Mammalian neurons, however, often express diverse types of ion channels, each with multiple states and multiple temperature-sensitive rate constants (Mitsuiye et al. 1997; Rodriguez et al. 1998). Electrophysiological studies of mammalian tissue in slices are done over a wide range of temperatures, 22–37°C, often with the assumption that the properties reflect those of the neurons in vivo but the influence of temperature has been examined systematically in only few slice preparations (Griffin and Boulant 1995; Volgushev et al. 2000). We show how the macroscopic currents of octopus cells in the mammalian cochlear nucleus vary over the range of temperatures generally used and that, because they respond differently to changes in temperature, electrophysiological properties of neurons are distorted at reduced temperatures.

The conductances measured in octopus cells in vitro account for their function not only in vitro but also in vivo. The temporal precision with which octopus cells convey acoustic information is made possible by their low input resistances at rest (~6 MΩ) that allow them to respond to synaptic activation of the auditory nerve with sharply timed action potentials (Oertel et al. 2000). In vivo they fire in phase with loud tonal stimuli at every cycle up to frequencies of 800/s, but at higher frequencies, they fire only once at the onset of a tone (Godfrey et al. 1975; Rhode and Smith 1986). They respond sensitively to broadband, periodic stimuli, such as trains of clicks, with action potentials whose temporal jitter is ~100 μs (Oertel et al. 2000). They fire only if synaptic inputs are synchronous and the rate of depolarization is high (Ferragamo and Oertel 2002; Golding et al. 1995).

The low input resistance of octopus cells results from the partial activation of a hyperpolarization-activated, mixed-cation conductance, $g_h$, and a low-voltage-activated potassium conductance, $g_{KL}$ (Bal and Oertel 2000, 2001). Depolarizing current pulses evoke only a single, small action potential, and hyperpolarizing current pulses evoke voltage changes that sag back toward rest (Golding et al. 1995, 1999). Octopus cells also have a high-voltage-activated potassium conductance, as well as a tetrodotoxin (TTX)-sensitive sodium conductance, and a high-voltage-activated calcium conductance, but these can generally not be clamped by controlling the voltage at the cell body (Bal and Oertel 2001). The present results show that the three conductances that can be studied by voltage clamp of the cell body are affected differently by temperature.

## METHODS

### *Preparation of slices*

Recordings were made from coronal slices of the most caudal region of the cochlear nuclear complex from mice (ICR strain) between 17 and 20 days old. Slices were made as reported previously (Bal and Oertel 2000). They were cut in normal physiological saline that contained (in mM) 130 NaCl, 3 KCl, 1.2 $KH_2PO_4$, 2.4 $CaCl_2$, 1.3 $MgSO_4$, 20 $NaHCO_3$, 3 HEPES, 10 glucose, saturated with 95% $O_2$-5% $CO_2$, pH 7.4, at between 24 and 27°C. All chemicals were from Sigma, unless stated otherwise. Slices, 200 μm thick, were cut using a vibrating microtome (Leica VT 1000S) and then were incubated in a holding chamber between 30 and 40 min at 33°C. They were then transferred to the recording chamber that was mounted on the stage of a compound microscope (Zeiss Axioskop) and viewed

Address for reprint requests and other correspondence: D. Oertel, Dept. of Physiology, University of Wisconsin Medical School, 1300 University Ave., Madison, WI 53706 (E-mail: oertel@physiology.wisc.edu).

The costs of publication of this article were defrayed in part by the payment of page charges. The article must therefore be hereby marked "*advertisement*" in accordance with 18 U.S.C. Section 1734 solely to indicate this fact.

through a ×63 water-immersion objective. Recordings were generally made within 2 h after they were cut.

### *Control of temperature*

When mounted in the microscope, slices in the recording chamber (volume of ~500 μl) were superfused at between 4 and 6 ml/min with physiological saline that was oxygenated in the reservoir whence it came. Temperature was regulated by controlling the temperature of the saline that was superfused over the tissue. Except when experiments required reducing the temperature, the saline in the reservoir was preheated in a water bath and fed by gravity to the recording chamber. The temperature was measured in the recording chamber, between the inflow of the chamber and the tissue, with a Thermalert thermometer (Physitemp) the input of which comes from a small thermistor (IT-23, Physitemp, diameter: 0.1 mm). The output of the Thermalert thermometer was fed into a custom-made, feedback-controlled heater that heated the saline in glass tubing (1.5 mm) just before it reached the chamber. An adjustable delay in the controller for the heater prevented oscillations. The lower temperature was limited by room temperature and varied between 22.4 and 23°C. Intermediate temperatures varied between 26.5 and 27°C. The high temperatures were kept between 33.1 and 33.4°C. It took ~2 min for the temperature to stabilize after a change was made.

### *Electrophysiological recordings*

Patch-clamp recordings were made with pipettes made from borosilicate glass whose resistances ranged between 5 and 6 MΩ. They were filled with a solution consisting of (in mM) 108 potassium gluconate, 9 HEPES, 9 EGTA, 4.5 $MgCl_2$, 14 phosphocreatinine (tris salt), 4 ATP (Na salt), and 0.3 GTP (tris salt). The pH was adjusted to 7.4 with KOH and was stable as the temperature was varied between 23 and 33°C. Recordings were made with an Axopatch 200A amplifier (Axon Instruments). Records were digitized at 50 kHz and low-pass filtered at 10 kHz. For measurements of large currents to be accurate and stable over relatively long time periods, it was essential that the series resistance was compensated and did not change during the experiment. Recordings in which the series resistance could not be compensated to ≥95% or in which the series resistance changed significantly (evident in the current transients at the onset and offset of voltage pulses) were eliminated from this study. The series resistance was 10.8 ± 3.4 MΩ ($n = 40$). With average membrane capacitance of 66.4 ± 18.8 pF ($n = 26$) in octopus cells, the time constant of the imposed voltage step was therefore on average 36 μs. The output was digitized through a Digidata 1320A (Axon Instruments) and fed into a computer. Stimulation and recording was controlled by pClamp 8 software (Axon Instruments).

To study their temperature dependence, currents were separated as reported previously (Bal and Oertel 2000, 2001). The control solution contained (in mM) 138 NaCl; 4.2 KCl, 2.4 $CaCl_2$, 1.3 $MgCl_2$, 10 HEPES, and 10 glucose, pH 7.4 and saturated with 100% $O_2$. The pH of this solution was stable over the range of temperatures used. In voltage-clamp experiments the voltage-sensitive sodium current was blocked by 1 μM tetrodotoxin (TTX), the voltage-sensitive calcium current was blocked by 0.25 mM $CdCl_2$ and synaptic currents were blocked with 40 μM 6,7-dinitroquinoxaline-2,3-dione (DNQX; Tocris Cookson, UK). In some experiments, 50 μM ZD7288 (Bal and Oertel 2000), and in some 60 nM α-dendrotoxin (α-DTX; Alomone Labs, Israel), was added to the control solution. Measurements of $I_h$ were made in an extracellular saline in which 5 mM 4-aminopyridine (4-AP) and 10 mM TEA were substituted for NaCl. All reported voltages were compensated for a –12 mV junction potential. Analyses were conducted off-line. Exponential fits to current traces were made with Clampfit software (Axon Instruments). To avoid contamination by the capacitative current, the first 4–4.5 ms after a voltage step were excluded from the fits. Fit intervals were between 0.5 and 1 s. Statistical analyses with Minitab (e-academy), and fits to the Boltzmann equation, $g/g_{max} = 1 - 1/[1 + \exp(V - V_{1/2})/\kappa]$, were made using Origin software (version 7.5).

## RESULTS

Recordings from 138 octopus cells that were ≥30 min in duration and the holding currents of which were <0.2 nA at –60 mV form the basis of this study. Octopus cells occupy the most dorsal and posterior tail of the VCN. This teardrop-shaped area contains only octopus cells that are separated from one another by fascicles of myelinated fibers. The myelinated fibers make the octopus cell area so dense that cell bodies are difficult to see under Nomarski optics; the bright cell bodies contrast with the dark fiber fascicles when they are illuminated under bright field with the field diaphragm closed to a pinpoint. After the recording was initiated, a physiological identification of octopus cells was made on the basis of their characteristic responses to current pulses (Bal and Oertel 2000, 2001; Golding et al. 1995, 1999).

We varied the temperature according to either of two protocols that are illustrated in the Fig. 1, *A* and *B*. To compare conductances in a single cell at several temperatures, transient

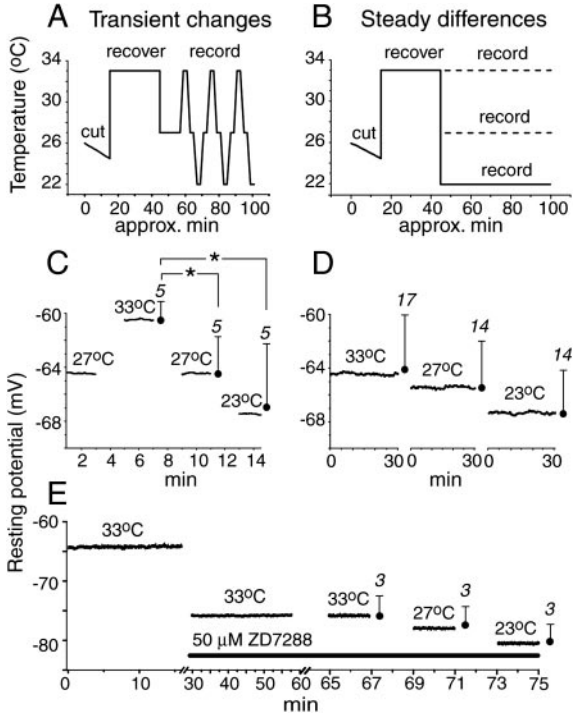


FIG. 1. Temperature affects resting potentials. *A*: to compare responses to changes in temperature in a single cell, a whole cell patch recording was initially made at 27°C. The temperature was then changed transiently so that comparisons could be made in measurements from a single cell. *B*: recordings were also made at different steady temperatures. Comparisons in these recordings had to be made between cells. *C*: traces are of the resting potential of 1 cell changed as the temperature was varied. *D*: resting potentials measured in separate cells that were held at differing temperatures differed less but in a similar direction as with transient changes. *E*: the addition of 50 μM ZD7288 hyperpolarized the resting potential in the same cell by ~12 mV. When $I_h$ was blocked in that cell, changes in temperature caused small changes of the resting potential. *C–E*: average values are indicated with dots (●). In this and all subsequent figures, bars (●) indicate the SD of the mean, the numbers in *italics* indicate the number of cells from which measurements were made, a single asterisk (*) indicates that bracketed values are significantly different at $P < 0.05$, and a double asterisk (**) indicates that values differ at $P < 0.001$.

changes were made (Fig. 1*A*). In other experiments, recordings in any one cell were made at a single, steady temperature and comparisons were made between cells (Fig. 1*B*).

### *Resting potential*

When the temperature was changed upward or downward from 27°C, the resting potentials of octopus cells changed. They depolarized with increases and hyperpolarized with decreases in temperature. The changes were initially large and then drifted back toward the earlier level over tens of minutes (not illustrated directly). The traces in Fig. 1*C* illustrate changes in the resting potential of a single cell as the temperature was changed transiently. When the cell was subjected to transient changes in temperature between 23 and 33°C, the resting potential shifted over 7 mV. The differences in resting potential were smaller when comparisons were made between cells that were held at differing steady temperatures. The traces in Fig. 1*D* show resting potentials in three separate recordings, each at a different temperature. On average, resting potentials differed by 6.5 mV when temperature changes were transient (Fig. 1*C*) and by 3.5 mV among cells held at 23 and 33°C (Fig. 1*D*). Differences between transient and steady manipulations of temperature reflect the drift of the resting potential back toward the original level. Changes in resting potential associated with transient changes in temperature were statistically significantly different from one another ($P < 0.05$; Fig. 1*C*).

At the resting potential, both inward $g_h$ and outward $g_{KL}$ are partly activated (Oertel et al. 2000). The finding that the magnitude of $I_h$ not only varies but also adapts to temperature changes (described in the following text) raised the question whether $I_h$ contributes to the adaptation in the resting potential. Figure 1*E* shows that addition of 50 $\mu$M ZD7288 to the bath hyperpolarized octopus cells by ~12 mV and that changes in temperature caused small changes of the resting potential (4 mV) that did not drift back toward the original level. The magnitude of differences in resting potential in individual cells as a function of temperature in the presence of ZD7288 was similar to the magnitude of differences between cells held at different steady temperatures.

### *Action potentials*

Depolarizing current pulses each evoke only a single action potential in octopus cells (Golding et al. 1995). The action potentials, though small, are conventional in that they have thresholds and are tetrodotoxin-sensitive (Golding et al. 1999). Action potentials evoked from rest by depolarizing current pulses were taller and broader at lower than at higher temperature. Changes in temperature affected the amplitude of action potentials, measured as the voltage difference between the visually identified threshold and the peak, and their duration, measured as the width of the action potential at the threshold (Fig. 2*A*). Superimposed action potentials from a recording of one cell in which the temperature was changed transiently (Fig. 2*B*) showed a similar relationship as the shapes of action potentials in separate cells that were recorded at differing steady temperatures (Fig. 2*C*) and are reflected in the mean values given in the bar graphs.

### *Conductances*

Octopus cells have several voltage-sensitive conductances that are activated over a wide range of voltages. Hyperpolarization between about –35 and –100 mV activates a mixed cation conductance, $g_h$, that is sensitive to 50 $\mu$M ZD7288 and has a reversal potential of –38 mV (Bal and Oertel 2000). Depolarization between about –70 and 0 mV, activates an $\alpha$-DTX-sensitive $K^+$ conductance, $g_{KL}$ (Bal and Oertel 2001). Octopus cells also have an $\alpha$-dendrotoxin-insensitive, TEA-sensitive $K^+$ conductance, $g_{KH}$, that activates at higher voltages, between about −40 and +20 mV. When other conductances are blocked, a voltage- and $Cd^{2+}$-sensitive inward current can be resolved that shows that octopus cells also have a voltage-sensitive $Ca^{2+}$ conductance (Bal and Oertel 2001). Octopus cells have TTX-sensitive $Na^+$ channels many of which are presumably in the axon because the voltage-sensitive $Na^+$ current can generally not be well clamped from the cell body (Bal and Oertel 2001; Golding et al. 1999). The influence of temperature on conductances that can be reasonably well measured in octopus cells, $g_h$, $g_{KL}$, and $g_{KH}$, is described in the following text.

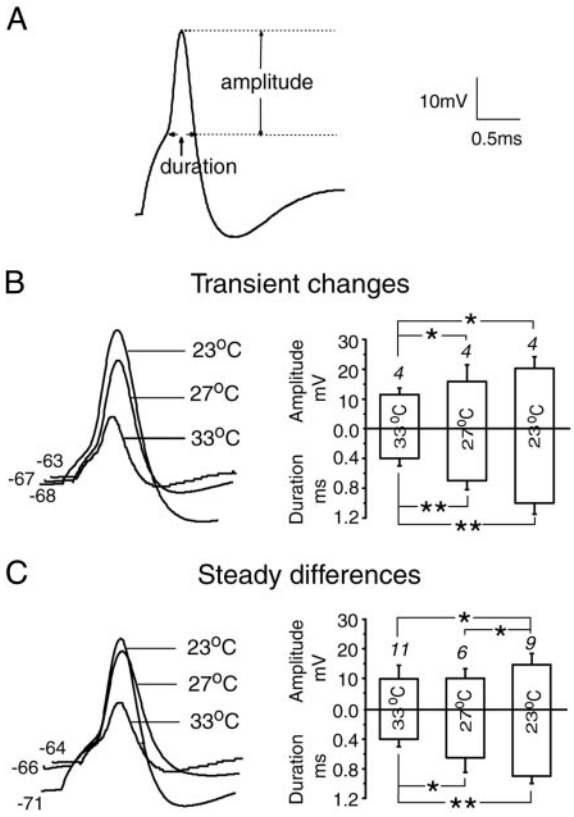


FIG. 2. Action potentials became smaller and briefer with increases in temperature, independent of whether the temperature was changed transiently or steadily. *A*: the amplitude and duration of action potentials evoked by current pulses were measured relative to the visually identified threshold. *B*: action potentials in a cell that was subjected to transient changes in temperature are superimposed so that peaks and thresholds are aligned in time and voltage, respectively. Resting potentials are given in millivolts at the *left* of the traces. Bar graphs on the *right* give mean ± SD. *C*: action potentials in 3 cells held at differing temperatures are superimposed so that the peaks and thresholds of action potentials are aligned.

### *Low-voltage-activated $K^+$ current ($I_{KL}$) is sensitive to temperature*

Depolarizing voltage steps from a holding potential of –90 to more than –70 mV evoked outward currents ($I_{KL}$). Recordings

of $I_{KL}$ were made in the presence of 1 $\mu$M TTX, 0.25 mM $Cd^{2+}$, 50 $\mu$M ZD7288, and 40 $\mu$M DNQX to block $g_{Na}$, $g_{Ca}$, $g_h$ and spontaneous synaptic currents, respectively. Figure 3, *A–C*, shows families of currents evoked by voltage steps from –90 to –40 mV recorded from three cells that were held at differing steady temperatures. The currents increased steeply in amplitude with steps to more depolarized potentials and then partially inactivated to a lower steady-state value. Currents were smaller at lower temperatures; a 10°C reduction from 33 to 23°C reduced the average peak $I_{KL}$ by almost two-thirds (Fig. 3*D*). Only a small fraction of that reduction can be attributed to the temperature sensitivity of $E_K$; if salts in the bath and pipette solutions are totally dissociated, $E_K$ would be expected to shift from –85 to –82 mV over this temperature range. The ratio of the peak current at 33°C to that at 23°C provides an estimate of the $Q_{10}$; at –40 mV the $Q_{10}$ was 2.6. It was impossible to measure the kinetics of activation and deactivation of $I_{KL}$ because the charging and discharging of the membrane obscured some of its time course. Inactivation was described by two exponential functions; fast and slow time constants had a $Q_{10}$ of 3.8 and 4, respectively (Fig. 3*E*; Table 1).

To measure $g_{KL}$ over its entire voltage range of activation, required that $I_{KL}$ be reduced (because large depolarizing voltages evoked currents that were so large that they saturated the amplifier) and that $I_{KL}$ be separated from $I_{KH}$ (Bal and Oertel 2001). Low concentrations of $\alpha$-DTX were used to reduce currents. $I_{KL}$ was evoked with steps to –40 mV and then 8 nM $\alpha$-DTX was applied. The ratio of the peak current in the presence and absence of 8 nM $\alpha$-DTX indicated what fraction

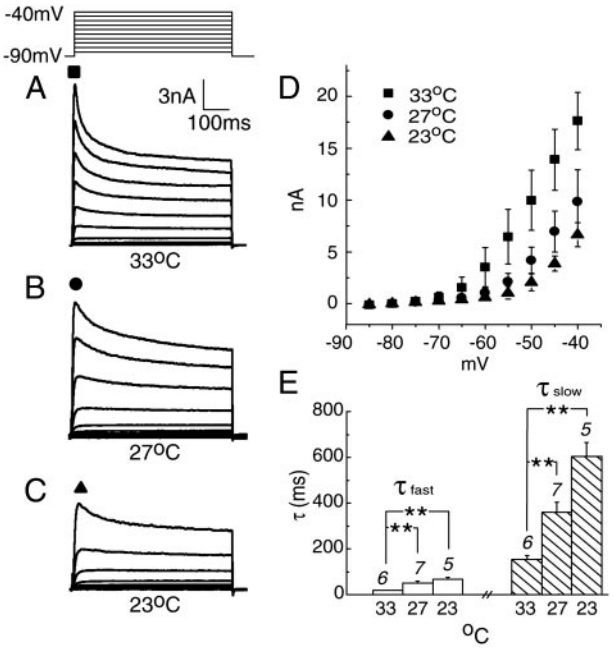


FIG. 3. Peak amplitude of low-voltage-activated $K^+$ current ($I_{KL}$) is sensitive to temperature. *A–C*: currents in 3 cells were evoked by voltage steps from –90 to –40 mV in +5-mV steps at various steady temperatures. The higher the temperature, the higher were the peak amplitudes and the rates of inactivation. Over most of this voltage range the contribution of $I_{KH}$ is small. *D*: average peak $I_{KL}$ ± SD is plotted as a function of voltage. *E*: bar graphs show mean ± SD of the fast ($\tau_f$) and slow ($\tau_s$) time constants as a function of temperature. Recordings were made in the presence of 1 $\mu$M TTX, 0.25 mM $Cd^{2+}$, 40 $\mu$M 6,7-dinitroquinoxaline-2,3-dione (DNQX), and 50 $\mu$M ZD7288.

TABLE 1. *Temperature sensitivity of potassium currents at steady temperatures*

| | 23°C | 33°C | ≈$Q_{10}$ |
|---|---|---|---|
| $I_{KL}$ | | | |
| Peak *I* (nA) −40 mV | 6.7 ± 1.2 *(5)* | 17.6 ± 2.8 *(6)* | 2.6 |
| ≈ max *g*KL (nS) −5 mV | 253 ± 66 *(4)* | 506 ± 183 *(4)* | 2 |
| Inact. $\tau_f$, (ms) −45 mV | 68 ± 8 (40%) *(5)* | 18 ± 1.4 (67%) *(6)* | 3.8 |
| Inact. $\tau_s$, (ms) −45 mV | 605 ± 61 (60%) *(5)* | 153 ± 17 (33%) *(6)* | 4 |
| DTX-K-s | | | |
| Peak *I* (nA) −40 mV | 2.6 ± 0.6 *(4)* | 7.6 ± 1.0 *(4)* | 2.9 |
| DTX-K-i | | | |
| Peak *I* (nA) −40 mV | 4.8 ± 1.3 *(4)* | 5.9 ± 1.0 *(4)* | 1.2 |
| $I_{KH}$ | | | |
| Peak *I* (nA) +5 mV | 13.7 ± 1.1 *(3)* | 12.4 ± 1.7 *(3)* | 0.9 |
| $V_{1/2}$ (mV) | −19 ± 3 *(3)* | −18 ± 3 *(3)* | 1 |
| Inact. $\tau$ (ms) 0 mV | 151 ± 17 *(3)* | 70 ± 9 *(3)* | 4.7 |

The properties of low ($I_{KL}$) and high-voltage activated $I_{KH}$ potassium currents are presented as means ± SD with italicized numbers in brackets indicating the number of measurements. The relative amplitudes associated with the fast ($\tau_f$) and slow ($\tau_f$) time constants are shown in parentheses. DTX-K-s and DTX-K-i denote dendrotoxin K-sensitive and -insensitive currents. $Q_{10}$ = (value at 33°C)/(value at 23°C), with $1/\tau$ used to calculate $Q_{10}$ for time constants.

of the peak $I_{KL}$ was blocked by 8 nM $\alpha$-DTX. The sensitivity of $I_{KL}$ to higher concentrations of $\alpha$-DTX was used to separate $I_{KL}$ from $I_{KH}$. One such experiment done at 27°C is illustrated in Fig. 4, *A–C*. Figure 4*A* shows that $I_{KL}$ was reduced by 8 nM $\alpha$-DTX. Although the action of $\alpha$-DTX is considered to be voltage independent (Hopkins et al. 1999), the peak currents were reduced more than the steady-state currents; the ratio of the peak current in the absence and presence of 8 nM $\alpha$-DTX was 3.1 while that of the steady-state currents at the end of the pulse was 2.7. The following analysis was done using peak values. In the same cell and in the continued presence of 8 nM $\alpha$-DTX, voltage steps to 0 mV evoked mixed high- and low-voltage activated currents, which were subsequently separated by blocking $I_{KL}$ with 60 nM $\alpha$-DTX and leaving $I_{KH}$. The difference in currents measured in the absence and presence of 60 nM $\alpha$-DTX was the reduced $I_{KL}$ (Fig. 4*B*). Application of the correction factor 3.1 revealed the maximum, peak $g_{KL}$. The voltage-sensitivity of the peak $g_{KL}$ was derived from the relationship $g_{KL} = I_{KL}/(V_m - E_K)$ where *g* is conductance, *I* is current, $V_m$ is membrane potential, and $E_K$ is the $K^+$ equilibrium potential. In this cell, $g_{KL}$ was fully activated at –20 mV (Fig. 4*C*). The shapes of the *g-V* functions varied; the voltage at which activation saturated was near –20 mV in some cells, as in Fig. 4*C*, but in others saturation was sloping. A similar variability was also noted in a previous study (Bal and Oertel 2001). One explanation for these results is that at least some of $g_{KL}$ is electrically distant from the cell body and is not well clamped. We know therefore that quantitative measures of this conductance are imperfect estimates. To compare them, maximal conductances were estimated from the peak current evoked by pulses to –5 mV. These were significantly lower at 23 and 27°C than at 33°C (Fig. 4*D*), having a $Q_{10}$ of ~2.

We compared how two pharmacologically distinct components of $I_{KL}$ were affected by temperature. The sensitivity of $I_{KL}$ to $\alpha$-DTX, a peptide toxin derived from the venom of green mamba snakes, indicated that this current was mediated through ion channels of the Kv1 family (Bal and Oertel 2001; Glazebrook et al. 2002; Harvey 1997; Hopkins 1998; Hopkins

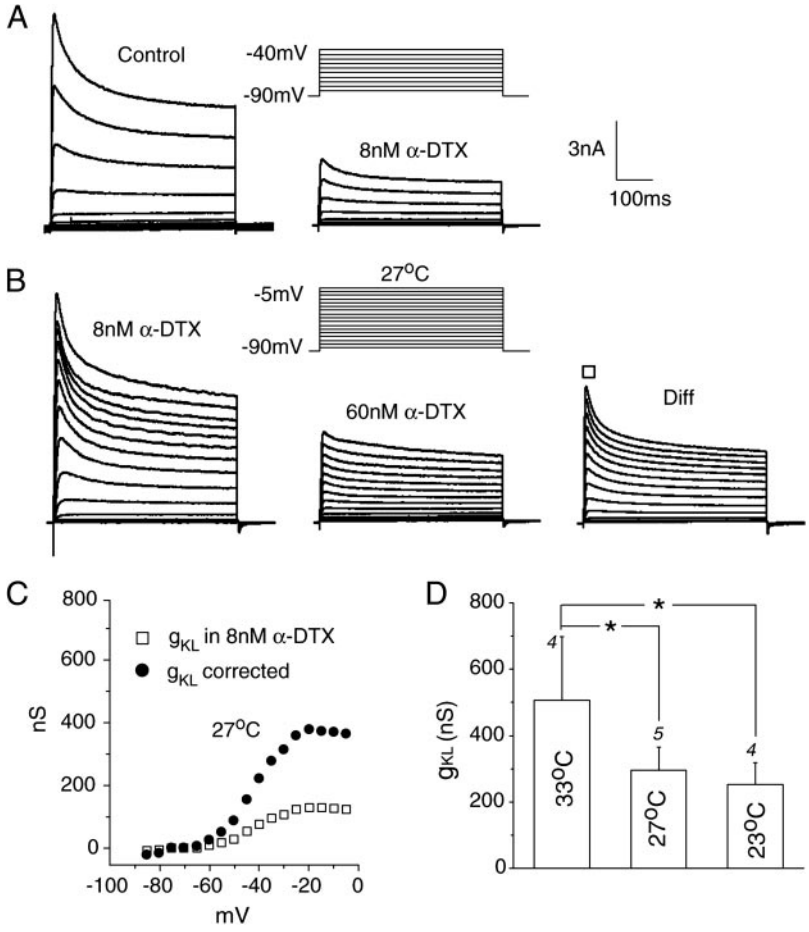


FIG. 4. The maximum amplitude of $g_{KL}$ differed as a function of temperature. Measurements required that the currents be reduced and separated from $g_{KH}$. *A*: $I_{KL}$ was first measured over relatively negative voltages, −90 to −40 mV, in the range where $I_{KH}$ is activated weakly. Then 8 nM α-dendrotoxin-K (α-DTX) was applied to reduce the large current. In this cell, the peak current at −45 mV was reduced by a factor of 3.1. *B*: in the same cell and in the continued presence of 8 nM α-DTX, voltage steps to 0 mV evoked further outward currents. To separate $I_{KH}$ from $I_{KL}$ 60 nM α-DTX was added to block $I_{KL}$ fully. The remaining current was $I_{KH}$; the difference current before and after the application of 60 nM α-DTX was the reduced $I_{KL}$. *C*: to measure the voltage-dependence of $g_{KL}$, $g_{KL}$ was calculated from $I_{KL}$ according to Ohm's law, $g_{KL} = I_{KL}/(V_m - E_K)$. $E_K$ was taken to be –77 mV, the reversal potential of this current measured in a previous study (Bal and Oertel 2001). The correction factor 3.1 that was measured in *A* for peak current was applied to obtain the maximum $g_{KL}$. *D*: comparison of the α-DTX-sensitive conductance, $g_{KL}$, at –5 mV at various temperatures. Recordings were made in the presence of 1 μM TTX, 0.25 mM $Cd^{2+}$, 40 μM DNQX, and 50 μM ZD7288.

et al. 1994; Owen et al. 1997; Stühmer et al. 1989). Dendrotoxin-K (DTX-K), derived from the venom of black mamba snakes, blocks channels that contain at least one Kv1.1 α subunit (Robertson et al. 1996; Wang et al. 1999). In octopus cells, essentially all $I_{KL}$ was blocked by α-DTX but only part was blocked by DTX-K, indicating that some, but not all, channels that mediate $I_{KL}$ contain Kv1.1 subunits (Bal and Oertel 2001). We examined whether the part of $I_{KL}$ that is sensitive to DTX-K is affected by temperature similarly or differently from that which is not sensitive to DTX-K. A comparison of the difference currents illustrated in Fig. 5, *A* and *B*, shows that the peak of the DTX-K-sensitive current is reduced and that inactivation is slowed at low temperature. Current-voltage plots of the mean peaks of the DTX-K-sensitive current (Fig. 5*C*) and -insensitive current (Fig. 5*D*) show that both components of $I_{KL}$ were reduced at low temperature. The reduction in the peak was more prominent in the DTX-K-sensitive current. The reduction in the peak DTX-K sensitive current, but not the DTX-K-insensitive current measured as the $Q_{10}$, was >1.3, the value expected from a diffusion-mediated current on purely physical grounds. The $Q_{10}$ values are summarized in Table 1.

### *High-voltage-activated $K^+$ current ($I_{KH}$) is insensitive to temperature*

In octopus cells the α-DTX-insensitive $K^+$ current, $I_{KH}$, is activated at more depolarized voltages than the α-DTX-sensitive $K^+$ current, $I_{KL}$ (Bal and Oertel 2001). In the presence of 60 nM α-DTX, 1 μM TTX, 0.25 mM $Cd^{2+}$, 50 μM ZD7288 and 40 μM DNQX to suppress $I_{KL}$, $I_{Na}$, $I_{Ca}$, $I_h$ and spontaneous miniature synaptic currents respectively, the voltage could be stepped from a holding potential of –90 to +15 mV (Fig. 6, *A* and *B*). The resulting outward currents had a voltage range of activation that began at about −40 mV (Fig. 6*C*). The peak currents did not vary significantly with temperature (Fig. 6*C*). The kinetics of the activation and inactivation, were however sensitive to temperature. While we could not measure the rate of activation, the time to peak was slower at lower temperature. Single-exponential fits to the rate of inactivation showed that the time constant of inactivation was significantly faster at higher temperatures (Fig. 6*D*), having a $Q_{10}$ of 4.7 (Table 1). This finding suggests that the increase in diffusion-mediated current through the pore is balanced by changes in gating.

### *Differences in steady temperature affected the kinetics but not the maximum amplitude or voltage sensitivity of the hyperpolarization-activated current ($I_h$)*

Measurements of $I_h$ were made in the presence of 5 mM 4-aminopyridine (4-AP), 10 mM TEA, 1 μM TTX, 0.25 mM $Cd^{2+}$, and 40 μM DNQX to block $I_{KL}$, $I_{KH}$, $I_{Na}$, $I_{Ca}$, and spontaneous miniature synaptic currents, respectively (Bal and Oertel 2000). Under these conditions, >90% of the inward current is sensitive to ZD7288 and $Cs^+$ (Bal and Oertel 2001). The traces illustrated in Fig. 7, *A–C*, show families of currents evoked by identical voltage pulses in three different cells that

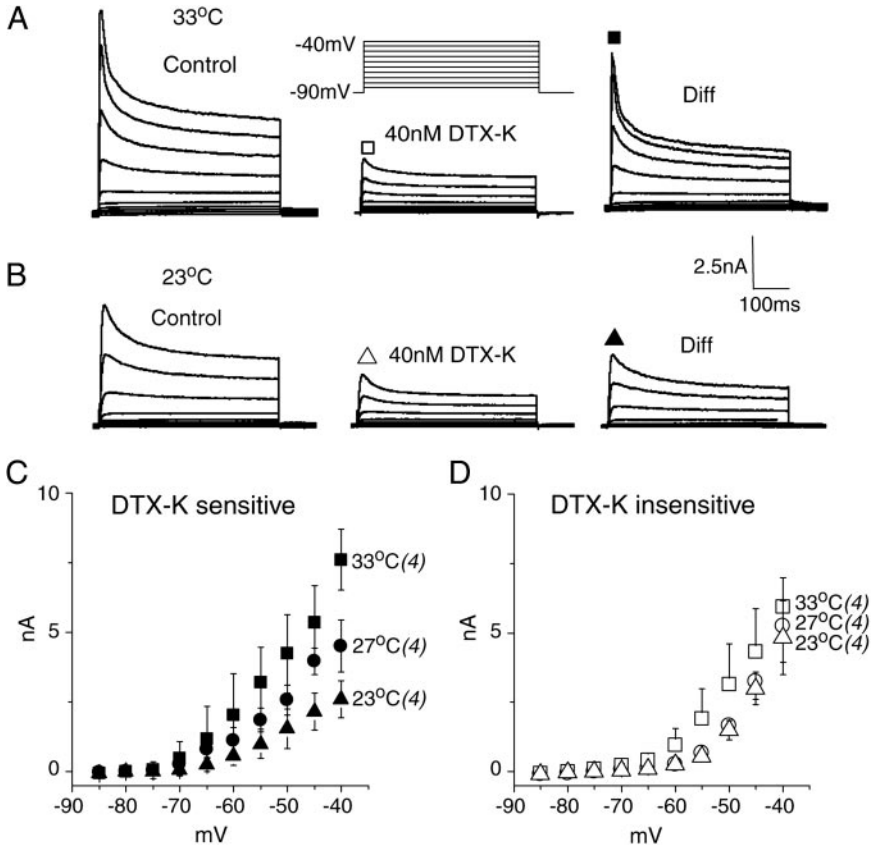


FIG. 5. Channels both with and without Kv1.1 subunits are sensitive to steady differences in temperature. DTX-K is a blocker of $K^+$ channels that contain at least one Kv1.1$\alpha$ subunit (Robertson et al. 1996; Wang et al. 1999). *A*: response to a family of voltage steps from a holding voltage of –90 to–40 mV in 5-mV increments at 33°C were recorded first in the absence and then in the presence of 40 nM DTX-K. The DTX-K-insensitive current (*middle*) is through channels that lack Kv1.1 subunits; subtraction of the DTX-K-insensitive currents from the control currents, the difference current (*right*) shows the current through channels that contain a Kv1.1 subunit. *B*: as in *A*, voltage steps from –90 to –40mV were applied in the absence and presence of 40 nM DTX-K at 23°C. *C*: current-voltage relationship of DTX-K-sensitive currents shows the mean ± SD derived from recordings at various temperatures. *D*: current-voltage relationship of DTX-K-insensitive currents in those same cells. Currents were measured in the presence of 1 $\mu$M TTX, 0.25 mM $Cd^{2+}$, 40 $\mu$M DNQX, and 50 $\mu$M ZD7288.

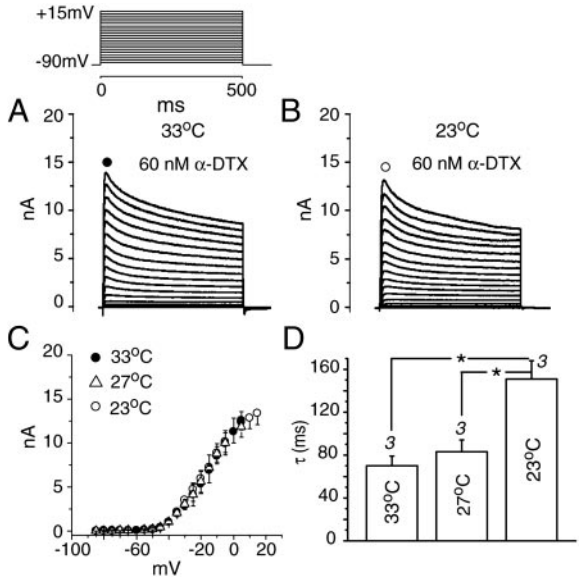


FIG. 6. Variation in temperature alters the kinetics but not the peak amplitude of the $\alpha$-DTX-insensitive, high-voltage-activated current, $I_{KH}$. *A*: family of currents evoked by depolarizing steps from –90 to +15 mV in 5-mV increments in the presence of 60 nM $\alpha$-DTX at 33°C. *B*: similar currents measured at 23°C in a different cell. *C*: the mean amplitude of peak currents ± SD as a function of voltage for $I_{KH}$ varied little with temperature. *D*: single-exponential fits to the time course of inactivation of currents evoked by voltage pulses to 0 mV revealed significant differences in the kinetics of $I_{KH}$ as a function of temperature. Recordings were made in the presence of 60 nM $\alpha$-DTX, 1 $\mu$M TTX, 0.25 mM $Cd^{2+}$, 50 $\mu$M ZD7288, and 40 $\mu$M DNQX to suppress $I_{KL}$, $I_{Na}$, $I_{Ca}$, $I_h$, and spontaneous miniature synaptic currents, respectively.

were maintained at differing temperatures. The slow rise in inward current evoked by hyperpolarizing voltage pulses reflects the activation of $I_h$. Because $g_h$ was partially activated at rest, depolarizing voltage pulses resulted in a deactivation of $I_h$.

The amplitude and voltage-dependence of $I_h$ did not vary with steady temperature but the kinetics were sensitive to temperature. The mean amplitude of $I_h$ at the end of a 1,100 ms-voltage pulse, each measured in four or five cells, was indistinguishable at three different steady temperatures (Fig. 7*D*). The voltage sensitivity of $g_h$ was measured from the tail currents after the voltage was stepped from between –25 and –115 to –77 mV, a value close to the reversal potential of $K^+$ currents (Bal and Oertel 2000). This plot shows that there is no significant difference in the voltage-sensitivity of $g_h$ as a function of the steady temperature (Fig. 7*E*). The rates of activation, however, were sensitive to voltage as well as temperature, with $Q_{10}$s between 1.8 and 4.6 (Table 2). The values of the fast ($\tau_{fast}$) and slow ($\tau_{slow}$) time constants were faster at higher temperature; a comparison of responses to –105 mV are illustrated in Fig. 7*F*. The relative amplitude of the fast time constant was also between 10 and 20% larger at 33 than at 23°C over the voltage range between –70 and –105 mV. Deactivation, too, was faster at higher temperature. Deactivation followed a single exponential time course whose time constant was slowed from about 130 ms at 33°C to 300 ms at 23°C. The results are summarized in Table 2.

### *Transient changes in temperature altered not only the kinetics but also the amplitude of $I_h$*

The consequences of transient temperature changes on $I_h$ are illustrated in Fig. 8. The recording from the octopus cell was

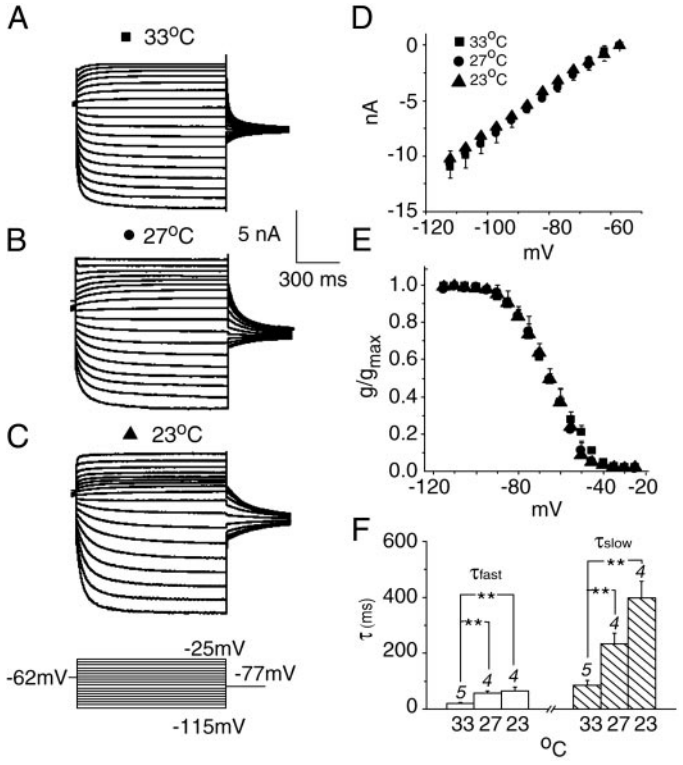


FIG. 7. Steady differences in temperature affect the kinetics, but not the amplitude, of the hyperpolarization-activated current, $I_h$. *A–C*: families of currents were evoked in separate cells that were held at different steady temperatures. The voltage steps are illustrated in the cartoon at the *bottom*. Both the activation and deactivation of currents was slower at lower than at higher temperatures. *D*: the amplitude of $I_h$ was not was not significantly affected by temperature. Plot shows mean ± SD of current at the end of the voltage pulses. *E*: plot of the amplitude of tail currents as a function of the voltage of the previous pulse reveals the voltage sensitivity of $g_h$. The half-activation voltage was −65 mV and did not vary significantly with temperature. *F*: activation of $I_h$ was fit well with double-exponential functions. Fast and slow time constants ($\tau$) varied with voltage and temperature. Bars show amplitudes of time constants at three temperatures in responses to voltage pulses to –105 mV; the amplitude of $\tau_{fast}$ was ~0.8. The numbers in *italics* show the number of cells from which measurements were made for *D–F*.

initiated at 27°C (Fig. 8*A*). Two minutes after the temperature was raised to 33°C, the traces shown in Fig. 8*B* were recorded. The currents activated more rapidly and to larger steady-state amplitudes at 33 than at 27°C. At the conclusion of those measurements, the temperature was lowered to 27°C (traces resembled those in Fig. 8*A* and are not shown). Thereafter the temperature was lowered to 23°C, left for 2 min, and currents were measured again. The currents were further slowed and reduced (Fig. 8*C*). Figure 8*D* shows a plot of the mean amplitude of currents at the end of the voltage step after transient temperature changes in four cells; steady-state currents were reduced over the entire voltage range at reduced temperatures while the instantaneous currents in those same traces did not change. The voltage-sensitivity of $g_h$ was similar at the three temperatures (Fig. 8*E*). The rates of activation were faster at higher than at lower temperatures. A comparison of fast and slow time constants of responses to pulses to –105 mV were larger and the relative contribution of the fast time constant was greater at higher temperatures (Fig. 8*F*) having a $Q_{10}$ of ~1.8. The rates of deactivation were also faster at higher temperature. The $Q_{10}$ values are summarized in Table 2.

Finding that the change in amplitude of $I_h$ that resulted from changes in temperature was transient, led us to examine the time course of these changes. The traces from one cell show that $I_h$ was reduced when the temperature was reduced to 23°C (Fig. 9, *A* and *B*). The activation rate of the currents remained slowed, but the steady-state amplitude adapted to the original levels within 10 min (Fig. 9*C*). A subsequent increase in temperature to 33°C caused the currents to activate more quickly but to similar levels (Fig. 9*D*). To illustrate the time course of the changes, steady-state responses to voltage steps from –55 to –100 mV were averaged in three cells and plotted (Fig. 9*E*). The amplitude of $I_h$ returned to the original value over ~15 min after a reduction of temperature from 33 to 23°C and over ~5 min after an increase in temperature but the kinetics did not adapt with time. The time constants and their relative weights were relatively stable at any one temperature even while the amplitude changed (Fig. 9*E, bottom*).

TABLE 2. *Temperature sensitivity of the hyperpolarization-activated current, $I_h$*

| | 23°C | | 33°C | | ≈$Q_{10}$ | |
|---|---|---|---|---|---|---|
| | Transient | Steady | Transient | Steady | Transient | Steady |
| Number of cells | 4 | 4 | 4 | 5 | | |
| $I_{ss}$, (nA) −115 mV | −7.2 ± 0.4 | −10.2 ± 1.8 | −11.0 ± 1.0 | −11.0 ± 1.4 | 1.5 | 1.0 |
| Act. $\tau_f$ (ms) −75 mV | 122 ± 16 | 175 ± 7 | 69 ± 10 | 41 ± 6 | 1.8 | 4.3 |
| Percentage | 50 | 40 | 60 | 73 | | |
| Act. $\tau_s$ (ms) −75 mV | 609 ± 41 | 674 ± 155 | 376 ± 40 | 193 ± 45 | 1.8 | 3.5 |
| Percentage | 50 | 60 | 40 | 27 | | |
| Act. $\tau_f$ (ms) −105 mV | 55 ± 6 | 65 ± 14 | 30 ± 7 | 20 ± 3 | 1.8 | 3.2 |
| Percentage | 70 | 73 | 81 | 85 | | |
| Act. $\tau_s$ (ms) −105 mV | 352 ± 39 | 398 ± 49 | 198 ± 31 | 86 ± 20 | 1.8 | 4.6 |
| Percentage | 30 | 27 | 19 | 15 | | |
| Deact. $\tau$ (ms) −115 to −77 mV | 282 ± 31 | 328 ± 40 | 181 ± 39 | 147 ± 24 | 1.6 | 2.1 |
| $V_{1/2}$ (mV) | −69 ± 2.4 | −65 ± 4.0 | −66 ± 2.1 | −65 ± 2.7 | 1 | 1 |
| $\kappa$ (mV) | 7.0 ± 0.8 | 9.7 ± 1.3 | 10 ± 1.0 | 10 ± 1.1 | 1.4 | 1 |

The properties of the hyperpolarization-activated conductance are presented as means ± SD. The relative amplitudes associated with the fast ($\tau_f$) and slow ($\tau_f$) time constants are shown in parentheses. For most properties $Q_{10}$ = (value at 33°C)/(value at 23°C). For time constants, the $Q_{10}$ = (value at 23°C)/(value at 33°C).

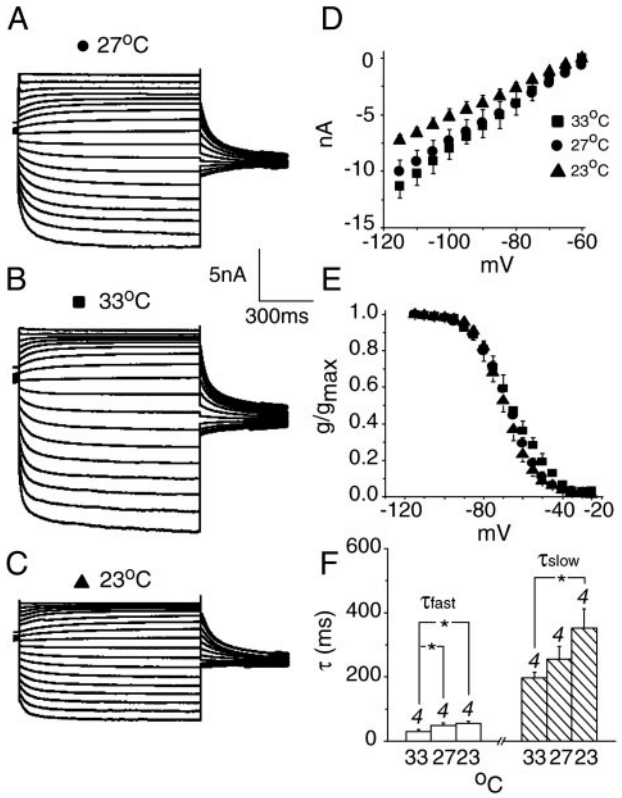


FIG. 8. Transient changes in temperature alter not only the kinetics but also the amplitude of $I_h$. *A–C*: recordings from 1 cell that initially was held at 27°C. The temperature was raised to 33°C; after ~2 min when the temperature stabilized, voltage pulses between –25 and –115 mV were used to evoke the family of currents in *A*. The temperature was then reduced to 27°C and a similar family of voltage pulses was used to evoke the currents shown in *B*. A further reduction was made in the temperature to 23°C and currents were measured again. In this cell, the steady-state $I_h$ was smaller when it was measured at low than at high temperature. *D*: current-voltage plot of steady-state currents shows that there is a consistent difference in the amplitude at the steady state with changes in temperature. In the same traces, there was no difference in the instantaneous current at the onset of the hyperpolarizing pulse (data not shown) indicating that at lower temperature, less $I_h$ was activated. *E*: voltage sensitivity of $g_h$, measured from tail currents, differed by 3 mV and was not statistically significant. *F*: the time course of activation was faster at higher than at lower temperature. Activation to –105 mV was fit with double-exponential functions. Both time constants, $\tau$, shortened with increasing temperature.

## DISCUSSION

Alterations in temperature affect the rates of diffusion through ion channels, the rates of conformational changes that lead to their activation and inactivation, and the rates of the biochemical reactions with which ion channels are modulated and transported into and out of membranes. The diverse consequences of changing temperature make it difficult to predict how cells will respond. While the rates at which conductances are activated, deactivated and inactivated are slower at lower temperatures, the amplitude of each of three major voltage-sensitive conductances in octopus cells is affected differently. Lowering the temperature from 33 to 23°C decreases the peak $g_{KL}$ but leaves the peak $g_{KH}$ unchanged. In octopus cells, resting potentials are more negative and action potentials are broader and taller at 23 than at 33°C. The smaller maximum $g_K$ seems to augment its slower activation to make action potentials taller and broader at depressed temperatures. An unexpected result was that the steady-state amplitude of $g_h$ that is activated by hyperpolarizing voltage pulses changes transiently and adapts over minutes to changes in temperature. The present results suggest that modulation of $g_h$ plays a role in regulating the resting potential of octopus cells because both the resting potential and $g_h$ itself adapt over tens of minutes when $g_h$ is present and the resting potential does not adapt when $g_h$ is blocked. These experiments indicate that electrophysiological properties of neurons are distorted when recordings are made at reduced temperature.

### *Conductances of octopus cells*

Several of the conductances of octopus cells have been identified and studied in sufficient detail that we could examine

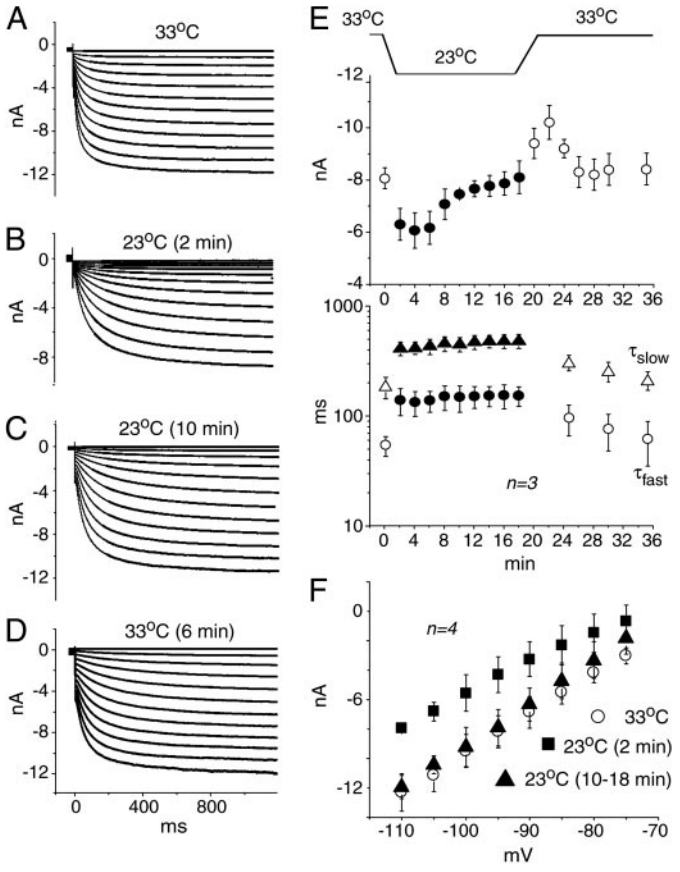


FIG. 9. The amplitude of $I_h$ is temporarily reduced with a reduction in temperature. *A*: the cell was initially held at 33°C while the voltage was stepped from –55 mV to a range of voltages between –55 and –110 mV. *B*: soon after the temperature was reduced to 23°C, the same voltage steps evoked currents that were slower and smaller. *C*: after 10 min at 23°C, the amplitude, but not the rates of activation, recovered. *D*: when the temperature was returned to 33°C, the rate of activation and amplitude increased (not shown). A few minutes later, the amplitude of $I_h$ fell back to its original value. *E*: mean amplitude of currents at the steady state (*top*) in responses to voltage pulses from –55 to –100 mV, recovered over a period of minutes after a reduction in temperature from 33 to 23°C. The amplitude of the steady-state current overshot its original value but stabilized at its original value within 5 min when the temperature was returned from 23 to 33°C. Unlike the amplitudes, the kinetics of activation did not adapt over time (*bottom*). In the same 3 cells, the mean slow (△) and fast (○) time constants of activation (fit to current traces of 1-s duration, of which only the 1st segments are illustrated in *A–D*) were slowed by a reduction in temperature and returned to their original values when the temperature was raised back to 33°C. *F*: current-voltage relationships of currents measured at the end of the hyperpolarizing voltage pulses show that the amplitude of currents was temporarily reduced by a reduction in the temperature.

how they are affected by differences in temperature. At rest, two large voltage-sensitive conductances, $g_{KL}$ and $g_h$, are partially activated. Octopus cells also have $g_{KH}$, and voltage-sensitive $Na^+$ and $Ca^{2+}$ conductances that are activated by strong depolarization (Bal and Oertel 2000, 2001; Golding et al. 1999).

The current mediated by $g_{KL}$ reverses near the theoretical $E_K$, begins to activate at about –70 mV, is half-maximally activated near –45 mV, and has a maximal conductance of, on average, 500 nS (Bal and Oertel 2001). The *g-V* curves sometimes show signs of imperfect voltage-clamp suggesting that it is located, at least in part, at sites electrically distant from the cell body, possibly in the axon.

Two lines of evidence indicate that $g_{KL}$ is mediated through $K^+$ channels of the Kv1 (also termed shaker-related or KCNA) family. First, $g_{KL}$ is blocked by toxins that act on Kv1 channels. $I_{KL}$ is sensitive to $\alpha$-DTX, which blocks channels that contain Kv1.1, Kv1.2, and Kv1.6 $\alpha$ subunits but does not distinguish among them (Dolly and Parcej 1996; Harvey 1997; Hopkins 1998; Owen et al. 1997; Stühmer et al. 1989). DTX-I resembles $\alpha$-DTX structurally (Gasparini et al. 1998) and also blocks $I_{KL}$ in neurons of auditory brain stem nuclei (Brew and Forsythe 1995; Dodson et al. 2002; Lu et al. 2004; Rathouz and Trussell 1998; Rothman and Manis 2003). $I_{KL}$ is partially blocked by tityustoxin K$\alpha$, specific for channels that contain Kv1.2 subunits (Hopkins 1998; Werkman et al. 1993), and by DTX-K, specific for channels that contain Kv1.1 subunits (Owen et al. 1997; Robertson et al. 1996; Wang et al. 1999). Second, Kv1.1, Kv1.2, and Kv1.4 subunits have been localized in the cochlear nuclei (Fonseca et al. 1998; Wang et al. 1994). In peripheral nerve, Kv1.1 channels have been localized in the perinodal region of axons (Wang et al. 1993).

The presence of $g_{KL}$ is common among neurons in brain stem nuclei that transmit acoustic information in the timing of their firing. It was initially described in mammalian bushy cells (Manis and Marx 1991; Rothman and Manis 2003). Similar conductances were later found in neurons of the medial nucleus of the trapezoid body (Brew and Forsythe 1995; Brew et al. 2003; Dodson et al. 2002; Forsythe and Barnes-Davies 1993), medial superior olive (Wu and Kelly 1991), ventral nucleus of the lateral lemniscus (Wu 1999), lateral superior olive (Barnes-Davies et al. 2004), homologues of bushy cells in avian nucleus magnocellularis (Lu et al. 2004; Rathouz and Trussell 1998) as well as in octopus cells (Bal and Oertel 2001; Golding et al. 1999).

There is no reason to think that temperature sensitivity in the affinity of blockers, $\alpha$-DTX and DTX-K, can account for the differences in $I_{KL}$ we observed at different temperatures. In octopus cells at 33°C, half-maximal blocking concentrations of $\alpha$-DTX and DTX-K were, 5 and 10 nM, respectively (Bal and Oertel 2001). Even if there had been a change in affinity of the blockers with temperature, the concentrations of $\alpha$-DTX (60 nM) and DTX-K (40 nM) used in the present study were in the saturating range so that small differences in the affinity with temperature would be expected to make only a small difference in the proportion of current blocked.

The temperature sensitivity of voltage-dependent currents was initially described in classical studies (Hodgkin and Huxley 1952a,c; Hodgkin et al. 1952). The amplitude of macroscopic and single channels that are probably largely Kv1.1 has a $Q_{10} \sim 1.45$, not far from the value 1.3 that is expected for aqueous diffusion (Koh and Vogel 1996). The time constants of activation of axonal $K^+$ channels, generally have larger $Q_{10}$s, like the $Q_{10}$ of inactivation in the present experiments, between 3 and 4 (Russ and Siemen 1996). The dependence on temperature of current flow through Kv1 channels that were expressed in oocytes shows that these channels undergo a series of transitions with differing temperature sensitivity, but the measurements were done on channels from which fast inactivation had been removed (Rodriguez et al. 1998). Together these results indicate that temperature sensitivity of peak $K^+$ currents in octopus cells reflects the temperature sensitivity of diffusion through the pore as well as the temperature sensitivity of activation and inactivation. In octopus cells, the low-voltage-activated current plays a key role in repolarization because in the presence of $\alpha$-dendrotoxin, action potentials are tall and of long duration (Bal and Oertel 2001; Ferragamo and Oertel 2002). It is likely that the amplitude of $I_{KL}$ is higher in situ than has been estimated from in studies in slices that were done at reduced temperature (Bal and Oertel 2001; Dodson et al. 2002; Forsythe and Barnes-Davies 1993; Manis and Marx 1991; Rathouz and Trussell 1998; Rothman and Manis 2003). The present results suggest that differences in the firing of action potentials between wild-type mice and those that lack Kv1.1 documented by Brew et al. (2003) in slices at room temperature may have been smaller than the differences that underlie the decrease in the temporal precision in responses to sound in vivo in those same cells in mice lacking Kv1.1 relative to wild-type mice (Kopp-Scheinpflug et al. 2003).

The $g_{KH}$ begins to activate at about –40 mV, is half-maximally activated at –16 mV, and peaks have a mean maximal conductance of 115 nS (Bal and Oertel 2001). Similar conductances have been described in other auditory neurons (Brew and Forsythe 1995; Rathouz and Trussell 1998). Some authors have subdivided $g_{KH}$ into two separate currents (Rothman and Manis 2003). Ion channels of the Kv3 family have been detected in the octopus cell area and may mediate part or all of $g_{KH}$ (Perney and Kaczmarek 1997). Contamination by capacitative artifacts prevented our resolving the temperature sensitivity of the kinetics of activation and deactivation of this current. Like the $K^+$ conductance of squid axons, the maximum amplitude of the conductance is unaffected by temperature (Hodgkin and Huxley 1952b). In the outward rectification of rat skeletal muscle, $Q_{10}$ values of time constants associated with the *n* parameter in a Hodgkin-Huxley model for activation varied between ~2 over 30–38°C and 6 over 1–10°C (Beam and Donaldson 1983).

Hyperpolarization activates $I_h$, a current that reverses at –38 mV and is thus inward at rest (Bal and Oertel 2000). It is blocked by ZD7288 at $\mu$M concentrations. In the brain, hyperpolarization-activated channels are tetramers composed of three subunits, HCN1, HCN2, and HCN4 (Robinson and Siegelbaum 2003; Santoro et al. 1998, 2000). Homomeric HCN1 channels activate most rapidly and are least modulated by cAMP (Santoro et al. 1998). HCN4 channels activate most slowly and both HCN2 and HCN4 channels are strongly modulated by cAMP (Ludwig et al. 1999; Seifert et al. 1999). HCN1 is expressed in the vicinity of the octopus cell area of the VCN; HCN2 and HCN4 are also present in the VCN but are distributed more diffusely (Notomi and Shigemoto 2004; Santoro et al. 2000). The distribution of HCN1 and HCN2 protein reveals strong labeling of octopus cells for both sub-

units but with different patterns. HCN1 appears to label the membranes of cell bodies and dendrites, whereas HCN2 appears to be localized in the cytoplasm (Koch et al. 2004). Heteromeric channels composed of HCN1 and HCN2 subunits are intermediate in their kinetics and sensitivity to cAMP (Chen et al. 2001; Ulens and Tytgat 2001). The fast and slow time constants of activation of $g_h$ at room temperature in octopus cells resemble those of heteromeric HCN1-HCN2 channels expressed in oocytes (Ulens and Tytgat 2001), but in their insensitivity to cAMP, these channels more closely resemble homomeric HCN1 channels (Bal and Oertel 2000).

The measurements of the temperature sensitivity of the kinetics of $I_h$ in the present study are consistent with earlier reports. In octopus cells, the $Q_{10}$ for the time constants of activation to about –100 mV is >3, as is the $Q_{10}$ for the activation of HCN1 and HCN4 channels expressed in COS cells (Ishii et al. 2001), and in the same range as Purkinje fibers of the heart (Hart 1983) and for the activation of $I_h$ in hippocampal pyramidal cells (Magee 1998; Santoro et al. 2000). The present experiments indicate that the voltage sensitivity of $I_h$ in octopus cells is unaffected by temperature. In Purkinje fibers of the heart (Hart 1983) and in cultured olfactory neurons (Vargas and Lucero 1999), elevation in temperature shifts the voltage sensitivity in the hyperpolarizing direction. In contrast, Watts et al. (1996) reported that the activation curve of $I_h$ in neurons of the *substantia nigra* shifts in the depolarizing direction with increases of temperature. However, as the voltage pulses in these studies were not long enough for currents consistently to reach steady-state activation, the shapes of voltage-activation curves contained distortions; at reduced temperatures, activation was slower and farther from the steady-state level than at higher temperature.

The observation was first made in the heart that $I_h$ has a high temperature dependence (DiFrancesco and Ojeda 1980; Hart 1983). Changes in the amplitude of $I_h$ are a prominent feature of the responses to cold of cold-sensitive sensory neurons in culture (Viana et al. 2002). In hippocampal pyramidal cells the amplitude of $I_h$ was reduced at steady, lower temperature, with a $Q_{10}$ of 1.95 (Magee 1998). None of these authors reports that the amplitude of $I_h$ adapts over tens of minutes.

Our experiments indicate that the amplitude of $I_h$ adapts after it changes with temperature. After an initial change in amplitude, the amplitude of $I_h$ returns to near the original value over a period of minutes. The adaptation in amplitude in the absence of corresponding changes in the rate of activation suggests that adaptation results from changes in the number of openable channels and points at possible mechanisms. Temperature could affect the trafficking of these channels to change their surface expression (Santoro et al. 2004). Accessory proteins can also modulate the amplitude of $I_h$. MinK-related protein 1, for example, acts as a $\beta$ subunit for HCN2 the presence of which increases $I_h$ without affecting its voltage sensitivity (Qu et al. 2004). Tyrosine kinase has been shown to increase hyperpolarization-activated currents without changing the voltage sensitivity (Wu and Cohen 1997). However, as this type of modulation occurs in heterologously expressed HCN4 channels, but not in HCN1 or HCN2 channels (Yu et al. 2004), it is unclear whether such a mechanism can obtain in octopus cells. Binding cyclic nucleotides to the C-terminal linker region stabilizes the open state of HCN2 channels, but, unlike increases in temperature, it also alters the voltage sensitivity of channels (Craven and Zagotta 2004; Shin et al. 2004).

### *Action potentials*

The consequences of changes of temperature on the shape of action potentials and on the overall electrical excitability reflect the effects of temperature on multiple voltage-dependent conductances and their interactions. It has been known since the 19th century that the symptoms of patients with multiple sclerosis are alleviated by reduced temperature (Uhthoff phenomenon). Reducing the temperature between 33 and 23°C made action potentials in octopus cells taller and broader. Presumably this resulted from the slower activation and smaller maximum amplitude of $g_{KL}$ just as a pharmacological reduction in $g_{KL}$ caused action potentials in octopus cells to become taller and broader (Bal and Oertel 2001; Ferragamo and Oertel 2002). In axons, it has been shown that the activation and inactivation of $Na^+$ channels by a voltage step are slowed and that the peak current is reduced by a reduction in temperature (Chiu et al. 1979). Action potentials are robust and prolonged at reduced temperatures because repolarizing currents are also slowed (Hodgkin and Huxley 1952a). Removing Kv1.1 in axons genetically results in only subtle changes at physiological temperature but at reduced temperatures motor axons become hyperexcitable and fire repetitively (Zhou et al. 1998). In visual cortical neurons, too, action potentials become taller and broader at room temperature than at 35°C (Volgushev et al. 2000). In MNTB neurons of the same Kv1.1- null mice, the higher input resistance reduced the current required to evoke action potentials and action potentials were broader but not taller (Brew et al. 2003). These findings are consistent with the conclusion from a model of bushy cells that $g_{KL}$ plays a key role in regulating repetitive firing while $g_{KH}$ is important for repolarizing individual action potentials (Rothman and Manis 2003). As blocking $g_{KL}$ in octopus cells disrupts the repolarization of action potentials, its role in repolarizing action potentials differs qualitatively from that in MNTB and bushy cells.

### *Resting potentials*

Both $I_h$ and $I_{KL}$ are activated at rest in octopus cells and thus contribute to setting the resting potential, but they are not its only determinants. The importance of $g_h$ in determining the resting potential has been pointed out for other cells, too (Robinson and Siegelbaum 2003). In hippocampal pyramidal cells, blocking $I_h$ caused a hyperpolarization of the resting potential of 3–4 mV (Magee 1998). Blocking $I_{KL}$ depolarized the resting potential by ~7 mV and blocking $I_h$ caused the resting potential to become hyperpolarized by 10 mV, on average (Bal and Oertel 2000, 2001; Oertel et al. 2000). As octopus cells are hyperpolarized with the reduction in temperature from 33 to 23°C and the resting potential adapts over a similar time course as $g_h$, it seems that the decrease in $g_h$ plays an important role in setting the resting potential. However, it is also clear that the control of the resting potential is not simply determined by $g_h$ and $g_{KL}$ because reducing the temperature hyperpolarizes octopus cells even when $g_h$ is blocked. The influence of temperature on the resting potential differs dramatically between neurons. In visual cortical cells, a reduction in temperature depolarized cells (Volgushev et al. 2000).

ACKNOWLEDGMENTS

We thank I. Siggelkow for support with histology and for keeping us supplied with physiological saline and R. Kochhar for keeping our computers running. We also thank M. McGinley and A. Rodrigues for lively discussions and for critically reading the manuscript. J. H. Wittig, Jr., made excellent criticisms of the manuscript. We are particularly grateful to three anonymous reviewers, each of whom made valuable suggestions that led to substantial changes and improvements.

GRANTS

The work was supported by a grant from the National Institute of Deafness and Other Communications Disorders Grant DC-00176.

REFERENCES

**Bal R and Oertel D.** Hyperpolarization-activated, mixed-cation current ($I_h$) in octopus cells of the mammalian cochlear nucleus. *J Neurophysiol* 84: 806–817, 2000.

**Bal R and Oertel D.** Potassium currents in octopus cells of the mammalian cochlear nuclei. *J Neurophysiol* 86: 2299–3211, 2001.

**Barnes-Davies M, Barker MC, Osmani F, and Forsythe ID.** Kv1 currents mediate a gradient of principal neuron excitability across the tonotopic axis in the rat lateral superior olive. *Eur J Neurosci* 19: 325–333, 2004.

**Beam KG and Donaldson PL.** A quantitative study of potassium channel kinetics in rat skeletal muscle from 1 to 37°C. *J Gen Physiol* 81: 485–512, 1983.

**Brew HM and Forsythe ID.** Two voltage-dependent $K^+$ conductances with complementary functions in postsynaptic integration at a central auditory synapse. *J Neurosci* 15: 8011–8022, 1995.

**Brew HM, Hallows JL, and Tempel BL.** Hyperexcitability and reduced low threshold potassium currents in auditory neurons of mice lacking the channel subunit Kv1.1. *J Physiol* 548: 1–20, 2003.

**Chen S, Wang J, and Siegelbaum SA.** Properties of hyperpolarization-activated pacemaker current defined by coassembly of HCN1 and HCN2 subunits and basal modulation by cyclic nucleotide. *J Gen Physiol* 117: 491–504, 2001.

**Chiu SY, Mrose HE, and Ritchie JM.** Anomalous temperature dependence of the sodium conductance in rabbit nerve compared with frog nerve. *Nature* 279: 327–328, 1979.

**Craven KB and Zagotta WN.** Salt bridges and gating in the COOH-terminal region of HCN2 and CNGA1 channels. *J Gen Physiol* 124: 663–677, 2004.

**DiFrancesco D and Ojeda C.** Properties of the current if in the sino-atrial node of the rabbit compared with those of the current iK, in Purkinje fibers. *J Physiol* 308: 353–367, 1980.

**Dodson PD, Barker MC, and Forsythe ID.** Two heteromeric Kv1 potassium channels differentially regulate action potential firing. *J Neurosci* 22: 6953–6961, 2002.

**Dolly JO and Parcej DN.** Molecular properties of voltage-gated $K^+$ channels. *J Bioenerg Biomembr* 28: 231–253, 1996.

**Ferragamo MJ and Oertel D.** Octopus cells of the mammalian ventral cochlear nucleus sense the rate of depolarization. *J Neurophysiol* 87: 2262–2270, 2002.

**Fonseca RC, Hallows JL, Trimmer JS, Rhodes KJ, and Tempel BL.** Localization of Kv channels in the auditory system. *Assoc Res Otolaryngol Abstr* 21: 213, 1998.

**Forsythe ID and Barnes-Davies M.** The binaural auditory pathway: membrane currents limiting multiple action potential generation in the rat medial nucleus of the trapezoid body. *Proc Roy Soc London B Biol Sci* 251: 143–150, 1993.

**Gasparini S, Danse JM, Lecoq A, Pinkasfeld S, Zinn-Justin S, Young LC, de Medeiros CC, Rowan EG, Harvey AL, and Menez A.** Delineation of the functional site of alpha-dendrotoxin. The functional topographies of dendrotoxins are different but share a conserved core with those of other Kv1 potassium channel-blocking toxins. *J Biol Chem* 273: 25393–25403, 1998.

**Glazebrook PA, Ramirez AN, Schild JH, Shieh CC, Doan T, Wible BA, and Kunze DL.** Potassium channels Kv1.1, Kv1.2 and Kv1.6 influence excitability of rat visceral sensory neurons. *J Physiol* 541: 467–482, 2002.

**Godfrey DA, Kiang NYS, and Norris BE.** Single unit activity in the posteroventral cochlear nucleus of the cat. *J Comp Neurol* 162: 247–268, 1975.

**Golding NL, Ferragamo MJ, and Oertel D.** Role of intrinsic conductances underlying responses to transients in octopus cells of the cochlear nucleus. *J Neurosci* 19: 2897–2905, 1999.

**Golding NL, Robertson D, and Oertel D.** Recordings from slices indicate that octopus cells of the cochlear nucleus detect coincident firing of auditory nerve fibers with temporal precision. *J Neurosci* 15: 3138–3153, 1995.

**Griffin JD and Boulant JA.** Temperature effects on membrane potential and input resistance in rat hypothalamic neurones. *J Physiol* 488: 407–418, 1995.

**Hart G.** The kinetics and temperature dependence of the pace-maker current if in sheep Purkinje fibers. *J Physiol* 337: 401–416, 1983.

**Harvey AL.** Recent studies on dendrotoxins and potassium ion channels. *Gen Pharmacol* 28: 7–12, 1997.

**Hodgkin AL and Huxley AF.** A quantitative description of membrane current and its application to conduction and excitation in nerve. *J Physiol* 117: 500–544, 1952a.

**Hodgkin AL and Huxley AF.** Currents carried by sodium and potassium ions through the membrane of the giant axon of *Loligo. J Physiol* 116: 449–472, 1952b.

**Hodgkin AL and Huxley AF.** The components of membrane conductance in the giant axon of *Loligo. J Physiol* 116: 473–496, 1952c.

**Hodgkin AL, Huxley AF, and Katz B.** Measurement of current-voltage relations in the membrane of the giant axon of *Loligo*. *J Physiol* 116: 424–448, 1952.

**Hopkins WF.** Toxin and subunit specificity of blocking affinity of three peptide toxins for heteromultimeric, voltage-gated potassium channels expressed in *Xenopus* oocytes. *J Pharmacol Exp Therap* 285: 1051–1060, 1998.

**Hopkins WF, Allen ML, Houamed KM, and Tempel BL.** Properties of voltage-gated $K^+$ currents expressed in Xenopus oocytes by mKv1.1, mKv1.2 and their heteromultimers as revealed by mutagenesis of the dendrotoxin-binding site in mKv1.1. *Pfluegers Eur J Physiol* 428: 382–390, 1994.

**Hopkins WF, Allen M, and Tempel BL.** Interactions of snake dendrotoxins with potassium channels. *Methods Enzymol* 294: 649–661, 1999.

**Ishii TM, Takano M, and Ohmori H.** Determinants of activation kinetics in mammalian hyperpolarization-activated cation channels. *J Physiol* 537: 93–100, 2001.

**Koch U, Braun M, Kapfer C, and Grothe B.** Distribution of HCN1 and HCN2 in rat auditory brain stem nuclei. *Eur J Neurosci* 20: 79–91, 2004.

**Koh D-S and Vogel W.** Single-channel analysis of a delayed rectifier $K^+$ channel in *Xenopus* myelinated nerve. *J Membr Biol* 149: 221–232, 1996.

**Kopp-Scheinpflug C, Fuchs K, Lippe WR, Tempel BL, and Rubsamen R.** Decreased temporal precision of auditory signaling in Kcna1-null mice: an electrophysiological study in vivo. *J Neurosci* 23: 9199–9207, 2003.

**Lu Y, Monsivais P, Tempel BL, and Rubel EW.** Activity-dependent regulation of the potassium channel subunits Kv1.1 and Kv3.1. *J Comp Neurol* 470: 93–106, 2004.

**Ludwig A, Zong X, Stieber J, Hullin R, Hofmann F, and Biel M.** Two pacemaker channels from human heart with profoundly different activation kinetics. *EMBO J* 18: 2323–2329, 1999.

**Magee JC.** Dendritic hyperpolarization-activated currents modify the integrative properties of hippocampal CA1 pyramidal neurons. *J Neurosci* 18: 7613–7624, 1998.

**Manis PB and Marx SO.** Outward currents in isolated ventral cochlear nucleus neurons. *J Neurosci* 11: 2865–2880, 1991.

**Mitsuiye T, Shinagawa Y, and Noma A.** Temperature dependence of the inward rectifier $K^+$ channel gating in guinea-pig ventricular cells. *Jpn J Physiol* 47: 73–79, 1997.

**Notomi T and Shigemoto R.** Immunohistochemical localization of Ih channel subunits, HCN1-4, in the rat brain. *J Comp Neurol* 471: 241–276, 2004.

**Oertel D, Bal R, Gardner SM, Smith PH, and Joris PX.** Detection of synchrony in the activity of auditory nerve fibers by octopus cells of the mammalian cochlear nucleus. *Proc Nat Acad Sci USA* 97: 11773–11779, 2000.

**Owen DG, Hall A, Stephens G, Stow J, and Robertson B.** The relative potencies of dendrotoxins as blockers of the cloned voltage-gated $K^+$ channel, mKv1.1 (MK-1), when stably expressed in Chinese hamster ovary cells. *Br J Pharmacol* 120: 1029–1034, 1997.

**Perney TM and Kaczmarek LK.** Localization of a high threshold potassium channel in the rat cochlear nucleus. *J Comp Neurol* 386: 178–202, 1997.

**Qu J, Kryukova Y, Potapova IA, Doronin SV, Larsen M, Krishnamurthy G, Cohen IS, and Robinson RB.** MiRP1 modulates HCN2 channel expression and gating in cardiac myocytes. *J Biol Chem* 279: 43497–43502, 2004.

**Rathouz M and Trussell L.** Characterization of outward currents in neurons of the avian nucleus magnocellularis. *J Neurophysiol* 80: 2824–2835, 1998.

**Rhode WS and Smith PH.** Encoding timing and intensity in the ventral cochlear nucleus of the cat. *J Neurophysiol* 56: 261–286, 1986.

**Robertson B, Owen D, Stow J, Butler C, and Newland C.** Novel effects of dendrotoxin homologues on subtypes of mammalian Kv1 potassium channels expressed in Xenopus oocytes. *FEBS Lett* 383: 26–30, 1996.

**Robinson RB and Siegelbaum SA.** Hyperpolarization-activated cation currents: from molecules to physiological function. *Annu Rev Physiol* 65: 453–480, 2003.

**Rodriguez BM, Sigg D, and Bezanilla F.** Voltage gating of *Shaker* $K^+$ channels; the effect of temperature on ionic and gating currents. *J Gen Physiol* 112: 223–242, 1998.

**Rothman JS and Manis PB.** Differential expression of three distinct potassium currents in the ventral cochlear nucleus. *J Neurophysiol* 89: 3070–3082, 2003.

**Russ U and Siemen D.** Kinetic parameters of the ionic currents in myelinated axons: characterization of temperature effects in a hibernator and a nonhibernator. *Pfluegers Eur J Phyiol* 431: 888–894, 1996.

**Santoro B, Chen S, Luthi A, Pavlidis P, Shumyatsky GP, Tibbs GR, and Siegelbaum SA.** Molecular and functional heterogeneity of hyperpolarization-activated pacemaker channels in the mouse CNS. *J Neurosci* 20: 5264–5275, 2000.

**Santoro B, Liu DT, Yao H, Bartsch D, Kandel ER, Siegelbaum SA, and Tibbs GR.** Identification of a gene encoding a hyperpolarization-activated pacemaker channel of brain. *Cell* 93: 717–729, 1998.

**Santoro B, Wainger BJ, and Siegelbaum SA.** Regulation of HCN channel surface expression by a novel C-terminal protein-protein interaction. *J Neurosci* 24: 10750–10762, 2004.

**Seifert R, Scholten A, Gauss R, Mincheva A, Lichter P, and Kaupp UB.** Molecular characterization of a slowly gating human hyperpolarization-activated channel predominantly expressed in thalamus, heart, and testis. *Proc Nat Acad Sci USA* 96: 9391–9396, 1999.

**Shin KS, Maertens C, Proenza C, Rothberg BS, and Yellen G.** Inactivation in HCN channels results from reclosure of the activation gate: desensitization to voltage. *Neuron* 41: 737–744, 2004.

**Stühmer W, Ruppersberg JP, Schroter KH, Sakmann B, Stocker M, Giese KP, Perschke A, Baumann A, and Pongs O.** Molecular basis of functional diversity of voltage-gated potassium channels in mammalian brain. *EMBO J* 8: 3235–3244, 1989.

**Ulens C and Tytgat J.** Gi- and Gs-coupled receptors up-regulate the cAMP cascade to modulate HCN2, but not HCN1 pacemaker channels. *Pfluegers-Eur J Physiol* 442: 928–942, 2001.

**Vargas G and Lucero MT.** Dopamine modulates inwardly rectifying hyperpolarization-activated current ($I_h$) in cultured rat olfactory receptor neurons. *J Neurophysiol* 81: 149–158, 1999.

**Viana F, De La PE, and Belmonte C.** Specificity of cold thermotransduction is determined by differential ionic channel expression. *Nat Neurosci* 5: 254–260, 2002.

**Volgushev M, Vidyasagar TR, Chistiakova M, Yousef T, and Eysel UT.** Membrane properties and spike generation in rat visual cortical cells during reversible cooling. *J Physiol* 522: 59–76, 2000.

**Wang FC, Bell N, Reid P, Smith LA, McIntosh P, Robertson B, and Dolly JO.** Identification of residues in dendrotoxin K responsible for its discrimination between neuronal $K^+$ channels containing Kv1.1 and 1.2 alpha subunits. *Eur J Biochem* 263: 222–229, 1999.

**Wang H, Kunkel DD, Martin TM, Schwartzkroin PA, and Tempel BL.** Heteromultimeric $K^+$ channels in terminal and juxtaparanodal regions of neurons. *Nature* 365: 75–79, 1993.

**Wang H, Kunkel DD, Schwartzkroin PA, and Tempel BL.** Localization of Kv1.1 and Kv1.2, two K channel proteins, to synaptic terminals, somata, and dendrites in the mouse brain. *J Neurosci* 14: 4588–4599, 1994.

**Watts AE, Williams JT, and Henderson G.** Baclofen inhibition of the hyperpolarization-activated cation current, $I_h$, in rat substantia nigra zona compacta neurons may be secondary to potassium current activation. *J Neurophysiol* 76: 2262–2270, 1996.

**Werkman TR, Gustafson TA, Rogowski RS, Blaustein MP, and Rogawski MA.** Tityustoxin-K alpha, a structurally novel and highly potent $K^+$ channel peptide toxin, interacts with the alpha-dendrotoxin binding site on the cloned Kv1.2 $K^+$ channel. *Mol Pharmacol* 44: 430–436, 1993.

**Wu JY and Cohen IS.** Tyrosine kinase inhibition reduces i(f) in rabbit sinoatrial node myocytes. *Pfluegers* 434: 509–514, 1997.

**Wu SH.** Physiological properties of neurons in the ventral nucleus of the lateral lemniscus of the rat: intrinsic membrane properties and synaptic responses. *J Neurophysiol* 81: 2862–2874, 1999.

**Wu SH and Kelly JB.** Physiological properties of neurons in the mouse superior olive: membrane characteristics and postsynaptic responses studied in vitro. *J Neurophysiol* 65: 230–246, 1991.

**Yu H-G Lu Z, Pan Z, and Cohen IS.** Tyrosine kinase inhibition differentially regulates heterologously expressed HCN channels. *Pfluegers Eur J Physiol* 447: 392–400, 2004.

**Zhou L, Zhang CL, Messing A, and Chiu SY.** Temperature-sensitive neuromuscular transmission in Kv1.1 null mice: role of potassium channels under the myelin sheath in young nerves. *J Neurosci* 18: 7200–7215, 1998.